ELSEVIER

Journal of Nuclear Materials 277 (2000) 82–90

journal of nuclear materials

www.elsevier.nl/locate/jnucmat

The niobium–silicon–uranium system

Tristan Lebihan[a,b], Peter Rogl[a,*], Henri Noël[b]

[a] *Institut für Physikalische Chemie der Universität Wien, Währingerstr. 42, A-1090 Vienna, Austria*
[b] *Laboratoire de Chimie du Solide et Inorganique Moléculaire, Université de Rennes I, C.N.R.S.-U.R.A. 1495, Avenue du Général Leclerc, F-35042 Rennes cedex, France*

Received 15 January 1999; accepted 8 June 1999

Abstract

Phase relations in the ternary system Nb–Si–U were established for the isothermal sections at 1000°C and 850°C. Experimental techniques used were optical microscopy, X-ray microanalyser (XMA) and X-ray powder analysis of arc melted samples which were annealed at 1000°C for 144 h and/or at 850°C for 300 h. Phase equilibria are characterised by the formation of two ternary compounds. Rietveld X-ray and neutron powder data refinements confirmed the stoichiometric behaviour for $U_2Nb_3Si_4$, and established isotypism with the ordered Zr_5Si_4-type ($Sc_2Re_3Si_4$-type). The second phase, $U_{2-x}Nb_{3+x}Si_4$,$x \simeq 0.25$, crystallises in the partially ordered Sm_5Ge_4-type ($Ce_2Sc_3Si_4$-type). At 1000°C both compounds form a narrow two-phase equilibrium. Due to the established two-phase equilibria: γ-(U,Nb) + $U_2Nb_3Si_4$ and Nb_5Si_3 + γ-(U,Nb) there is no compatibility between U_3Si_2 and niobium metal at 1000°C and at 850°C, respectively. $U_2Nb_3Si_4$ is weakly ferromagnetic below $T_c \simeq 35$ K. The remanence of only 0.0088 μ_B/U atom probably results from a non-linear antiferromagnetic structure, too weak to be discovered by neutron powder diffraction.

1. Introduction

In continuation of our systematic studies [1–3] of strong electron correlation in higher order intermetallics, we herein focused on the constitution, the structural chemistry and in particular on the occurrence of co-operative magnetism in 5f-element based ternary alloy systems with the early 4d-elements and silicon (transition from local-moment anti-ferromagnetism to a heavy fermion ground state). The present paper deals with the phase relations in the isothermal section of ternary system Nb–Si–U, with the crystal structure of the ternary compounds observed as well as with the magnetic behaviour of the novel phases in the temperature range from 1.4 to 300 K and in fields up to 2 T. As far as the phase equilibria are concerned, the research reported herein is related to low enriched uranium (LEU) proliferation resistant reactor fuel systems [4,5].

2. Experimental

Samples were usually of a total weight of 1 g and were prepared by argon arc-melting platelets of depleted uranium (claimed purity of (99.9%, supplied by Merck, Darmstadt, D) pieces of 6N-silicon (Alfa Ventron, Karlsruhe, D) and precompacted powders of niobium 99.9%, Metallwerk Plansee, A). The U-platelets were surface cleaned in diluted HNO_3 prior to melting. For homogeneity the samples were remelted several times and weight losses finally were less than 0.5 mass%. A part of each button was annealed at 1000°C on a W-substrate in a high vacuum furnace with a W-sheet thyristor-controlled heating system under a dynamic vacuum better than 10^{-4} Pa. After heat treatment the samples were cooled by switching off the power to the furnace. Most alloys particularly the uranium–rich alloys were also annealed at 850°C for 300 h. These

* Corresponding author. Tel.: +43-1 4277 52456; fax: +43-1 4277 9524.
E-mail address: peter.franz.rogl@univie.ac.at (P. Rogl).

0022-3115/00/$ - see front matter
PII: S0022-3115(99)00138-5

specimens were contained in a small alumina crucible and sealed under vacuum in a quartz tube, which after heat treatment was submersed in cold water.

Further details of sample preparation, of the X-ray techniques used as well as a general description of the magnetic measurements (SQUID-magnetometer) may be found from our preceding publication on binary uranium silicides [6].

Neutron powder diffraction in the temperature range from 1.5 to 120 K was performed at the ORPHEE 14 MW reactor (CEN-Saclay) using the G4-1 double-axis multicounter neutron powder diffractometer with a helium cryostat (wavelength $\lambda_n = 0.24268$ nm; resolution $\Delta d/d \geqslant 4\times10^{-3}$; see Ref. [7]). Preferred orientation effects were minimised by powdering the sample in a steel mortar to a grain size smaller than 30 μm. Further details concerning the experiment are summarised in Table 1. Precise atom parameters, occupation numbers, isotropic thermal factors and profile parameters were derived from a least squares full matrix Rietveld refinement routine [8] including simultaneous refinement of the background. Neutron scattering lengths were taken from a recent compilation by Sears [9]. The various reliability measures calculated are defined in Table 1 and equally apply to Rietveld refinements of X-ray powder diffraction data collected at room temperature from flat specimens in a D5000 automatic diffractometer.

The microstructures of uranium-rich alloys were inspected by optical microscopy on surfaces prepared by SiC-grinding and polishing the resin-mounted alloys with diamond pastes down to 1/4 μm grain size. Etching was effected by a mixture of 1 cm^3 HF + 5 cm^3 H_2O_2 in 94 cm^3 of H_2O. A CAMEBAX SX50 wavelength dispersive X-ray microanalyser (XMA) was used for proper identification of the phases and precipitates. Quantitative analyses were performed comparing the U-Mα_1, Nb-Lα_1 and the Si-Kα_1 emissions of the three elements in the alloys with those from elemental Nb or SiO_2 and UO_2 as reference materials applying the PAP correction procedure [10]. The experimental parameters employed were: 15 kV acceleration voltage, 15 to 20 nA sample current and spectrometer crystals such as PET for the U-Mα_1 and Nb-Lα_1 and TAP for the Si-Kα_1 radiation.

3. Results and discussion

3.1. The binary boundary systems

The binary boundary systems Nb–U and Nb–Si were accepted from a critical assessment of binary alloy phase diagrams by Massalski [11]. There are, however, minute changes for the isothermal reaction temperatures in a more recent compilation of the Nb–Si system by [12]. A reinvestigation of the binary Nb–Si compounds prepared from Sn or Cu flux is due to [13]. The U–Si used herein is the version established in a recent reinvestigation by the authors [6]. The uranium-rich part of the diagram up to 4 at.% Si is taken from Ref. [4]. A listing of the crystallographic data of the binary boundary phases is given in Table 2. Information on the magnetic

Table 1
Experimental data for Rietveld refinements of $U_2Nb_3Si_4$ ($Sc_2Re_3Si_4$-type)[a]

Parameter	Neutron data	X-ray data
Sample container	Aluminium cylinder, $\varnothing = 3$ mm	Flat specimen
Temperature (K)	1.4, helium cryostat	293
Radiation wavelength (nm)	$\lambda_n = 0.24268$	$\lambda_{Cu\,K\alpha} = 0.154056$
Absorption correction	$-0.1\times\sin 2\Theta$	–
Reactor, diffractometer	ORPHEE, CEN-Saclay	Siemens diffractometer D5000
Monochromator	pyrolitic graphite	Secondary monochromator (graphite)
Detector	800 cells, linear multidetector, BF_3	Scintillation counter
2Θ range (°)	3.03–82.93	13.00–100.00
Step-scan increment (2Θ)	0.10	0.02
Neutron coherent scattering lengths (fm), X-ray form factors	U: 8.417 Nb: 7.054 Si: 4.149	Hartree–Fock wave function
Number of contributing reflections	43	136
Background	interpolated, 6 background coefficients	Interpolated, 6 background coefficients
Preferred orientation	[0 0 1]	[0 0 1]
Number of variables	28	30
Biggest element of correlation matrix	0.8	0.86
Maximum Δ/σ	0.1	0.8

[a] Residual values: $R_e = [(N-P+C)/\sum \omega_i Y_i(\mathrm{obs})^2]^{1/2}$, $R_I = \sum |I_i(\mathrm{obs}) - (1/c)I_i(\mathrm{calc})| / \sum |I_i(\mathrm{obs})|$, $R_F = \sum |[I_i(\mathrm{obs})]^{1/2} - [I_i(\mathrm{calc})]^{1/2}| / \sum [I_i(\mathrm{obs})]^{1/2}$, $\chi^2 = (R_{\omega P}/R_e)^2$, $R_P = \sum |Y_i(\mathrm{obs}) - (1/c)Y_i(\mathrm{calc})| / \sum Y_i(\mathrm{obs})$, $R_{\omega P} = [\sum \omega_i |Y_i(\mathrm{obs}) - (1/c)Y_i(\mathrm{calc})|^2 / \sum \omega_i \ |Y_i(\mathrm{obs})|^2]^{1/2}$. Symbols used: I_i, integrated intensity of reflection i; ω_i, weighting function; Y_i, number of counts (background corrected at 2Θ); c, scale factor.

Table 2
Crystallographic data of the binary boundary phases of the U–Nb–Si system

Phase	Pearson symbol	Space group	Struktur-ber. Design.	Proto-type	Lattice parameters (nm)			Volume V (nm^3)	Comments	References
					a	b	c			
(Nb)	cI2	Im $\bar{3}$ m	A2	W	0.33004	...	...	0.0360	<2469°C	[11]
					0.32995	...	...	0.0359	at 1000°C	[12]
					0.3304	...	...	0.0361	Si-saturated ($\simeq$ 3 at.% Si)	[12]
(Si)	cF8	Fd $\bar{3}$ m	A4	$C_{diamond}$	0.54306	...	...	0.1602	<1414°C	[11]
(γ-U)	cI2	Im $\bar{3}$ m	A2	W	0.35335	...	...	0.0441	1135–774.8°C; at 787°C	[18]
					0.35498	...	...	0.0447	at 1000°C	[19]
(β-U)	tP30	$P4_2/mnm$	A_b	βU	1.07589	...	0.56531	0.6544	774.8 to 667.7°C	[18,19]
(α-U)	oC4	Cmcm	A20	αU	0.28537	0.58695	0.49548	0.0830	<667.7°C	[18,19]
Nb_3Si	tP32	$P4_2/n$	...	Ti_3P	1.0224	...	0.5189	0.5424	1975–1765°C	[12]
β-Nb_5Si_3	tI32	I4/mcm	$D8_m$	W_5Si_3	1.0018	...	0.5072	0.5090	2515–1645°C; 37.5–40.5 at.% Si	[12]
					0.997	...	0.508	0.5050	Si-rich	[12]
					1.0040	...	0.5081	0.5122	Nb-rich ?	[12]
α-Nb_5Si_3	tI32	I4/mcm	$D8_1$	Cr_5B_3	0.6571	...	1.1889	0.5133	<1935°C; 36.7–39.8 at.% Si	[12]
$NbSi_2$	hP9	$P6_222$	C40	$CrSi_2$	0.4819	...	0.6592	0.1326	<1935°C	[12]
					0.47834	...	0.65673	0.1301	Refined at R.T.	[20]
					0.4841	...	0.6658	0.1351	Refined at 1000°C	[20]
USi_3	cP4	Pm $\bar{3}$ m	$L1_2$	Cu_3Au	0.40353	...	...	0.0657	<1510°C	[11,6]
USi_2	tI12	$I4_1/amd$	C_c	$ThSi_2$	0.3922	...	1.4154	0.2171	<450°C (metastable)	[11,19]
USi_{2-x}	tI12	$I4_1/amd$	C_c	def-$ThSi_2$	0.39423	...	1.3712	0.2131	<1710°C, 65 at.% Si	[11,6]
USi_{2-x}	oI12	Imma	...	def-$GdSi_2$	0.3953	0.3929	1.3656	0.2121	at 64 at.% Si	[6]
U_3Si_5(o2)	oP6	Pmmm(?)	...	dist-$A1B_2$	0.3893	0.6717	0.4042	0.1057	at $\simeq$ 63 at.% Si	[6]
U_3Si_5(o1)	oP6	Pmmm(?)	...	dist-$A1B_2$	0.3864	0.6660	0.4073	0.1048	at 63 at.% Si	[6]
U_3Si_5(h)	hP3	P6/mmm	C32	def-$A1B_2$	0.38475	...	0.40740	0.0522	<1770°C	[11,6]
USi	tI138	14/mmm	...	USi	1.0587	...	2.4310	2.7247	<1580°C	[11,21]
USi	oP8	Pnma	B27	FeB	0.7585	0.3903	0.5663	0.1697	Impurity (O) stabilized [92Rem]	[11,19]

Table 2 (Continued)

Phase	Pearson symbol	Space group	Struktur-ber. Design.	Proto-type	Lattice parameters (nm)			Volume V (nm^3)	Comments	References
					a	b	c			
U_5Si_4	hP36	P6/mmm		$U_{20}Si_{14}C_3$	1.037	–	0.800	0.7726	<1100°C	[24]
U_3Si_2	tP10	P4/mbm	$D5_a$	U_3Si_2	0.73299	…	0.39004	0.2095	<1665°C	[11,19]
					0.73364	…	0.38900	0.2094		[6]
γ-U_3Si	cP4	$Pm\bar{3}$ m	$L1_2$	Cu_3Au	0.4346	…	…	0.0821	930–759°C; at 780°C	[4,19,22]
β-U_3Si	tI16	I4/mcm	$D0_c$	β-U_3Si	0.60328	…	0.86907	0.3163	762 to −153°C	[4,23,19]
α-U_3Si	oF32	Fmmm	…	α-U_3Si	0.8654	0.8549	0.8523	0.6306	<−153°C, at −193°C	[4,23,19]

behaviour of the binary uranium silicides is provided in [6]; magnetic data for the uranium–niobium solid solution are listed in the review article by Sechovsky and Havela [14].

3.2. The ternary system Nb–U–Si

3.2.1. Phase relations at 1000°C

Phase relations within the Nb–Si–U ternary system have been established for the complete isothermal section at 1000°C (Fig. 1), revealing two ternary compounds with close compositions: $U_2Nb_3Si_4$ crystallises in the ordered Zr_5Si_4-type ($Sc_2Re_3Si_4$-type, Ref. [15]) and $U_{2-x}Nb_{3+x}Si_4$, $x \simeq 0.25$, with the Sm_5Ge_4-type ($Ce_2Sc_3Si_4$-type, Ref. [16]) (see Table 3). At 1000°C both phases were observed to form a narrow two-phase equilibrium. Phase analyses and lattice parameters of a series of ternary alloys are listed in Table 3. From the variation of the lattice parameters in ternary three-phase alloys the existence of homogeneity ranges for the two modifications at 1000°C can be judged to be rather small (Table 3). This is in perfect agreement with the results of X-ray microanalyses on the alloys $U_{45}Nb_{25}Si_{30}$ and $U_{55}Nb_{10}Si_{35}$ annealed at 1000°C which confirmed the stoichiometric composition $U_{22.4}Nb_{33.9}Si_{43.7}$ for one phase ($Sc_2Re_3Si_4$-type) and an off-stoichiometric formula $U_{19.3}Nb_{37.4}Si_{43.3}$ (i.e., $U_{2-x}Nb_{3+x}Si_4$) for the second phase ($Ce_2Sc_3Si_4$-type). As seen from the micrograph of the annealed sample with the composition $U_{55}Nb_{10}Si_{35}$ (Fig. 2) both compounds tend to crystallise in long needles or plates which in many cases seem to precipitate along a common crystallographic plane. As most of the binary boundary phases engage in two-phase equilibria with stoichiometric $U_2Nb_3Si_4$, a relatively high thermodynamic stability of this ternary compound is in-

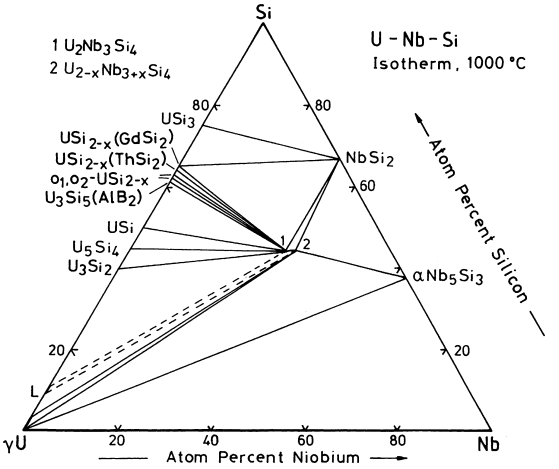

Fig. 1. Isothermal section at 1000°C of the Nb–Si–U system.

Table 3
Crystallographic data of ternary alloys U–Nb–Si annealed at 1000°C

Nominal compos. (at.%) U–Nb–Si	Phase	Space group	Proto-type	Lattice parameters (nm)			Volume V (nm^3)	c/a
				a	b	c		
12.5–12.5–75.0	$NbSi_2$	$P6_222$	$CrSi_2$	0.48009(6)	...	0.65948(6)	0.13163(3)	1.3737
	USi_3	Pm $\bar{3}$ m	Cu_3Au	0.40403(4)	...	...	0.06595(1)	1.0000
	Si	Fd $\bar{3}$ m	$C_{diamond}$	Traces	...	...	...	...
18.5–16.0–65.5	$NbSi_2$	$P6_222$	$CrSi_2$	0.47969(7)	...	0.6590(3)	0.1313(1)	1.3738
	$USi_{1.88}$	$I4_1/amd$	def-$ThSi_2$	0.3956(1)	...	1.3665(7)	0.2139(2)	3.4540
23.5–20.5–56.0	$NbSi_2$	$P6_222$	$CrSi_2$	0.4794(1)		0.6582(5)	0.1310(1)	1.3730
	$USi_{1.88}$	$I4_1/amd$	def-$ThSi_2$	0.39456(5)	...	1.3730(2)	0.2138(1)	3.4799
	$U_2Nb_3Si_4$	$P4_12_12$	$Sc_2Re_3Si_4$	0.7001(2)	...	1.2923(4)	0.6333(4)	1.8460
30.0–15.0–55.0	U_3Si_5(h)	P6/mmm	def-AlB_2	0.3848(2)	...	0.4071(3)	0.0522(1)	1.0578
	U_3Si_5(ol)	Pmmm(?)	dist-AlB_2	0.3876(2)	0.6672(4)	0.4067(3)	0.1052(1)	1.0491
	U_3Si_5(o2)	Pmmm(?)	dist-AlB_2	0.3886(3)	0.6739(6)	0.4030(3)	0.1056(1)	1.0372
	$U_2Nb_3Si_4$	$P4_12_12$	$Sc_2Re_3Si_4$	0.7019(2)	...	1.2959(8)	0.6384(5)	1.8463
40.0–10.0–50.0	U_3Si_5	P6/mmm	def-AlB_2	0.3850(1)	...	0.4069(8)	0.0522(2)	1.0568
	$U_2Nb_3Si_4$	$P4_12_12$	$Sc_2Re_3Si_4$	0.7048(1)	...	1.2983(8)	0.6450(5)	1.8421
	USi	I4/mmm	USi	1.0618(3)	...	2.4395(7)	2.7505(2)	2.2975
15.0–37.7–47.3	$U_{2-x}Nb_{3+x}Si_4$	Pnma	$Ce_2Sc_3Si_4$	0.6760(2)	1.3141(5)	0.6932(2)	0.6157(3)	1.0255
	$NbSi_2$	$P6_222$	$CrSi_2$	0.47966(7)		0.6590(2)	0.1313(1)	1.3740
	α-Nb_5Si_3	I4/mcm	Cr_5B_3	0.65765(5)	...	1.1911(1)	0.5150(1)	1.8108
40.0–15.0–45.0	$U_2Nb_3Si_4$	$P4_12_12$	$Sc_2Re_3Si_4$	0.7040(1)	...	1.2998(9)	0.6442(5)	1.8463
	USi	I4/mmm	USi	1.0609(6)	...	2.4371(7)	2.7431(3)	2.2971
	U_3Si_2	P4/mbm	U_3Si_2	0.7352(3)	...	0.3912(2)	0.2115(2)	0.5321
22.2–33.3–44.5	$U_2Nb_3Si_4$	$P4_12_12$	$Sc_2Re_3Si_4$	0.70389(1)	...	1.2984(1)	0.6433(1)	1.8446
35.0–25.0–40.0	$U_2Nb_3Si_4$	$P4_12_12$	$Sc_2Re_3Si_4$	0.7035(2)	...	1.2982(4)	0.6425(5)	1.8453
	U_3Si_2	P4/mbm	U_3Si_2	0.7345(1)	...	0.3899(1)	0.2103(1)	0.5309
	α-U	Cmcm	αU	0.2861(1)	0.5874(8)	0.4945(4)	0.0831(4)	1.7287
37.7–33.2–29.1	$U_2Nb_3Si_4$	$P4_12_12$	$Sc_2Re_3Si_4$	0.70332(6)	...	1.2982(4)	0.6421(2)	1.8458
	α-Nb_5Si_3	I4/mcm	Cr_5B_3	0.65771(9)	...	1.1888(3)	0.5143(2)	1.8075
	α-U	Cmcm	α-U	0.28593(5)	0.5875(4)	0.4949(2)	0.0831(1)	1.7309

ferred. Lattice parameters and unit cell dimensions of the boundary phases obtained from ternary multiphase alloys annealed at 1000°C compare well with those of the pure binary phases. This result backs the conclusion for small and in most cases negligible mutual solid solubilities among binary uranium and binary niobium silicides (see Table 3 and Fig. 1). This is particularly true for α-Nb_5Si_3 and U_3Si_2 which from XMA showed practically no solubility for uranium and niobium, respectively at 1000°C. Even in the as-cast alloys XMA revealed less than 0.6 at.% U in α-Nb_5Si_3 ($U_{0.6}Nb_{62.2}Si_{37.2}$) and less than 1.5 at.% Nb in U_3Si_2 ($U_{57.8}Nb_{1.5}Si_{40.7}$).Due to the generally very tough mechanical structure, silicon-poor alloys with less than 20 at.% Si revealed widely broadened and blurred X-ray reflections unsuitable to derive proper lattice parameters in order to determine the vertex of the γ-(U,Nb) + α-Nb_5Si_3 + $U_2Nb_3Si_4$ threephase field at the γ-(U,Nb) solution. Short term annealing of the heavily cold-worked fine powders in vacuum improved the quality of the X-ray recordings, however, γ-(U,Nb) was never present due to rapid decomposition below the monotectoid/eutectoid reaction temperature of the U-Nb binary revealing α-U instead. Optical and XMA inspection of the micrograph of the alloy $U_{45}Nb_{25}Si_{30}$ quenched from 1000°C (see Fig. 3) revealed the presence of the two phases $U_2Nb_3Si_4$, $U_{2-x}Nb_{3+x}Si_4$ and α-Nb_5Si_3 in a matrix of practically pure U dissolving about 1 at.% Nb and less than 0.1 at.% Si. Similarly the alloy $U_{55}Nb_{10}Si_{35}$ (annealed at 1000°C and quenched; Fig. 2) shows large grains of U_3Si_2 and plates of $U_2Nb_3Si_4$, $U_{2-x}Nb_{3+x}Si_4$ in a matrix of uranium which dissolved ca.0.5 at.% Si but practically no niobium. These results at first seem to be contradictory, however, according to the U–Si phase diagram [4], a small region of liquid phase appears near $U_{90}Si_{10}$ at 1000°C, which solidifies on quenching the samples giving raise to the non-equilibrium structures revealed in Figs. 2 and 3. From the observation of a two-phase equilibrium between α-Nb_5Si_3 and $U_{84.9}Nb_{15.0}Si_{0.1}$ in the alloy $U_{60}Nb_{30}Si_{10}$ at 1000°C as well as from the results obtained at 850°C (see below) it is therefore safely concluded that at 1000°C α-Nb_5Si_3 is in equilibrium with the full range of the γ-(U,Nb) solid solution (see Fig. 1).

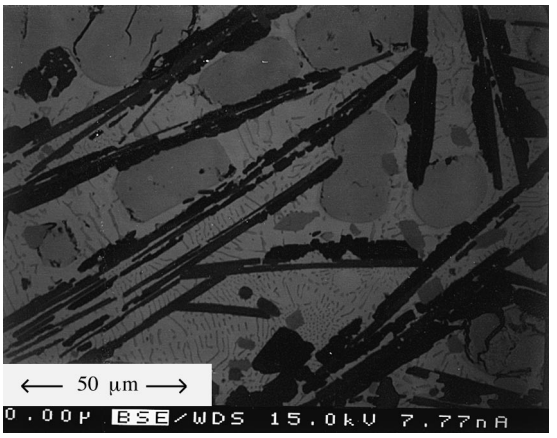

Fig. 2. Backscattered electron image of the alloy $U_{55}Nb_{10}Si_{35}$ annealed at 1000 °C. Dark plates or needles are $U_2Nb_3Si_4$ parallel to slightly brighter plates of $U_{2-x}Nb_{3+x}Si_4$. Large grey grains are U_3Si_2. Bright matrix is $U_{99.4}Nb_{0.1}Si_{0.5}$.

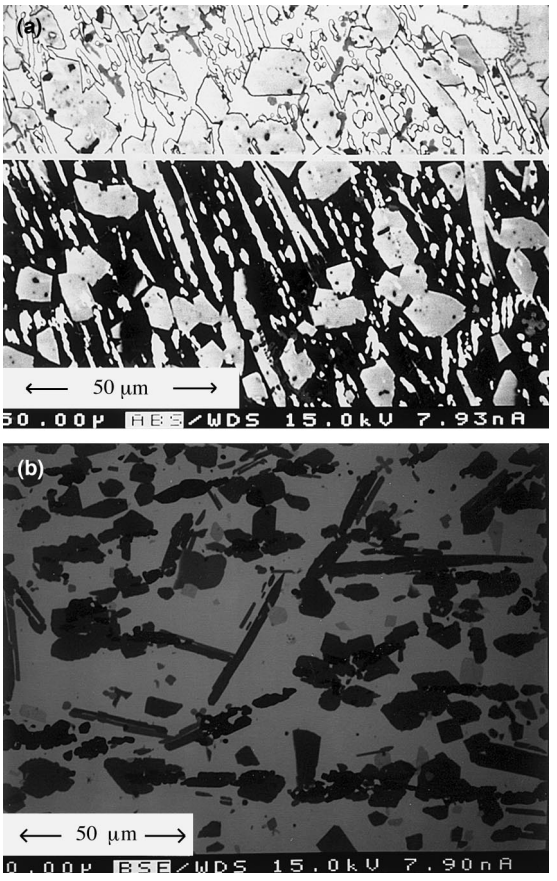

Fig. 3. Alloy $U_{45}Nb_{25}Si_{30}$, (*above*) absorbed electron image of as-cast alloy. Black square particles are Nb_5Si_3. Plates or needles are $U_2Nb_3Si_4$. Matrix is $U_{98.6}Nb_{1.5}Si_{0.1}$. (*below*) Backscattered electron image. Elongated dark particles are $U_2Nb_3Si_4$ and $U_{2-x}Nb_{3+x}Si_4$ (slightly brighter). Round dark particles are Nb_5Si_3. Matrix is $U_{98.9}Nb_{1.0}Si_{0.1}$.

3.2.2. Phase relations at 850°C

Evaluation of the samples annealed at 850°C by optical micrography, XMA and X-ray powder diffraction resulted in the phase distribution presented in Fig. 4. Again there is practically no solid solubility of Nb in U_3Si_2 ($U_{59.5}Nb_{0.1}Si_{40.4}$), in U_3Si ($U_{75.3}Nb_{0.1}Si_{24.6}$) and there are virtually no Si and Nb dissolved in the uranium-rich matrix ($U_{99.3}Nb_{0.6}Si_{0.1}$) in contact with the ternary phase $U_2Nb_3Si_4$ ($U_{21.4}Nb_{34.7}Si_{43.9}$). XMA also confirmed the three–phase equilibrium between uranium ($U_{99.3}Nb_{0.7}Si_{0.0}$), α-Nb_5Si_3 ($U_{1.0}Nb_{63.9}Si_{35.1}$) and ($U_2Nb_3Si_4$) ($U_{22.1}Nb_{34.1}Si_{43.8}$) (see Fig. 5). Equilibria in the uranium-poor regions of the diagram were checked on a few samples and were found to be consistent with the phase field distribution at 1000°C. The observation of $U_{2-x}Nb_{3+x}Si_4$ at 850°C, however, may be influenced

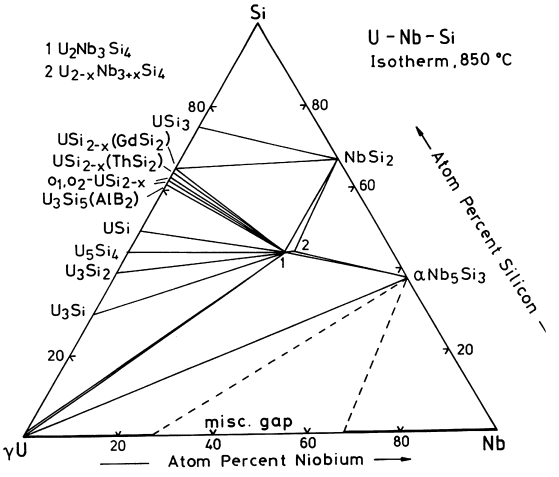

Fig. 4. Isothermal section at 850°C of the Nb–Si–U system.

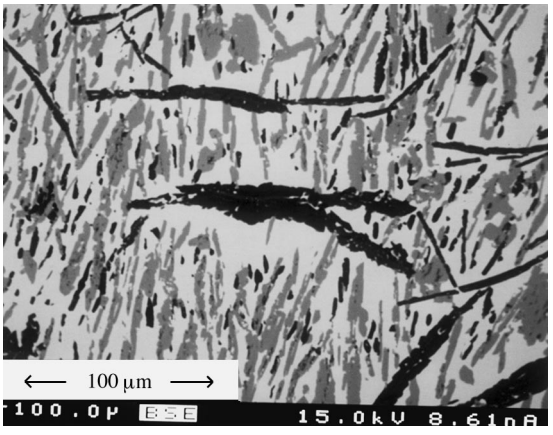

Fig. 5. Backscatter electron image of alloy $U_{54}Nb_{25}Si_{21}$, annealed at 850°C. Black particles are $U_2Nb_3Si_4$. Grey particles are Nb_5Si_3. Bright matrix is uranium ($U_{99.3}Nb_{0.7}Si_{0.0}$).

by retarded reaction kinetics due to slow diffusion mechanisms.

3.3. Powder X-ray and neutron Rietveld refinement of $U_2Nb_3Si_4$

3.3.1. Refinement of $U_2Nb_3Si_4$ with the ordered $Sc_2Re_3Si_4$-type

Room temperature X-ray powder patterns of $U_2Nb_3Si_4$ alloys, annealed and quenched from 1000°C, were successfully indexed on the basis of a primitive tetragonal unit cell (Table 4). Extinctions were observed only for the screw axes 4_1 and 2_1, $(0\,0\,l)$ and $(h\,0\,0)$ extinct for $l=4n+1$ and $h=2n+1$, respectively, and thus are compatible with $P4_12_12$ as the highest symmetric space group. The chemical formula, the unit cell dimensions, crystal symmetry and X-ray intensities strongly suggest isotypism with the ordered Zr_5Si_4-type ($Sc_2Re_3Si_4$-type; Ref. [15]). Assuming the atom order and the atom parameter set of $Sc_2Re_3Si_4$, a full matrix-full profile Rietveld refinement of a Siemens D5000 flat specimen intensity recording satisfactorily converged at a reasonably low residual value $R_F=0.046$ (Table 4, Fig. 6) and with only slightly modified atom parameters. The isotypism of $U_2Nb_3Si_4$ with the crystal structure of $Sc_2Re_3Si_4$ has been confirmed from a Rietveld refinement of a neutron powder profile recorded at 1.4 K (Table 4). Despite only a limited 2Θ range from 3° to 83° has been used at a long wavelength of $\lambda_n=0.24268$ nm, the precision obtained for the atom parameters unambiguously

Table 4
Crystallographic data for $U_2Nb_3Si_4$ ($Sc_2Re_3Si_4$-type) Space group: $P4_12_12$–D_4^4. No. 92, origin at 2_12

X-ray powder diffraction data at 295 K

$a=0.70389(1)$ nm, $c=1.29837(3)$ nm, $c/a=1.8446$, $V=0.6433$ nm^3

Atom	Site	x	y	z	Occ.	B_{iso} (nm^2)
U	8b	0.0029(4)	0.3357(4)	0.2182(1)	1.0	0.1
Nb1	8b	0.1580(7)	0.0020(7)	0.3772(6)	1.0	0.2
Si1	8b	0.2979(28)	0.0509(25)	0.1916(11)	1.0	0.3
Si2	8b	0.3779(25)	0.2854(30)	0.3195(12)	1.0	0.3
Nb2	4a	0.1726(10)	0.1726(10)	0.0	1.0	0.2

Reliability factors: $R_I=0.064$, $R_F=0.046$, $R_{\omega P}=0.097$, $R_e=0.051$, $\chi^2=1.90$

Neutron powder diffraction at 1.4 K

$a=0.7026(2)$ nm, $c=1.2950(6)$ nm, $c/a=1.8433$, $V=0.6392$ nm^3

Atom	Site	x	y	z	Occ.	B_{iso} (nm^2)
U	8b	0.995(3)	0.342(2)	0.2180(7)	1.0	0.1
Nb1	8b	0.165(2)	0.000(2)	0.370(2)	1.0	0.2
Si1	8b	0.295(5)	0.040(4)	0.183(2)	1.0	0.3
Si2	8b	0.377(5)	0.296(6)	0.329(2)	1.0	0.3
Nb2	4a	0.170(3)	0.170(3)	0.0	1.0	0.2

Reliability factors: $R_I=0.064$, $R_F=0.107$, $R_{\omega P}=0.058$, $R_e=0.016$, $\chi^2=13.2$

Interatomic distances (given in nm) within the first gap (as calculated from the X-ray data); standard deviations are generally less than 0.003 nm

U	1 U	0.3470	Nb1	1 Si2	0.2570	Si1	1 Si2	0.2408
	2 U	0.3635		1 Si1	0.2626		1 Nb1	0.2626
	1 Nb2	0.3282		1 Si2	0.2634		1 Nb1	0.2638
	1Nb1	0.3312		1 Si1	0.2638		1 Nb1	0.2723
	1 Nb2	0.3318		1 Si2	0.2675		1 Nb2	0.2775
	1 Nb1	0.3351		1 Si1	0.2723		1 Nb2	0.2776
	1 Si1	0.2858		1 Nb2	0.3077		1 U	0.2858
	1 Si2	0.2887		1 Nb2	0.3086		1 U	0.2907
	1 Si2	0.2902		1 U	0.3312		1 U	0.2927
	1 Si1	0.2907		1 U	0.3351			
	1 Si1	0.2927				Si2	1 Si1	0.2408
	1 Si2	0.2970	Nb2	2 Sil	0.2775		1 Nb1	0.2570
	1 Si2	0.3016		2 Sil	0.2776		1 Nb1	0.2634
				2 Si2	0.2893		1 Nb1	0.2675
				2 Nb1	0.3077		1 Nb2	0.2893
				2 Nb1	0.3086		1 U	0.2887
				2 U	0.3282		1 U	0.2902
				2 U	0.3318		1 U	0.2970
							1 U	0.3016

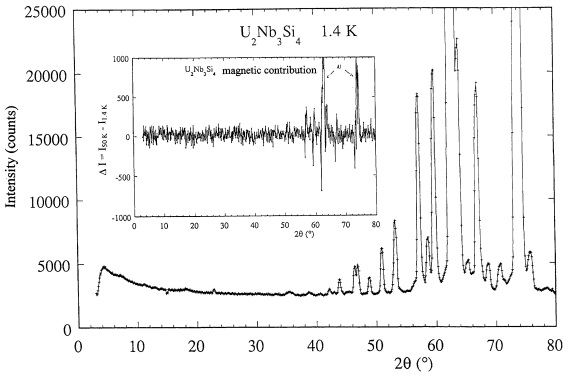

Fig. 6. Neutron powder diffraction profile for $U_2Nb_3Si_4$ ($Sc_2Re_3Si_4$-type). Inset: Neutron powder difference profile (1.4–50 K) revealing the absence of magnetic contributions (strongest nuclear peak $I_{(302)} = 20\,000$ counts).

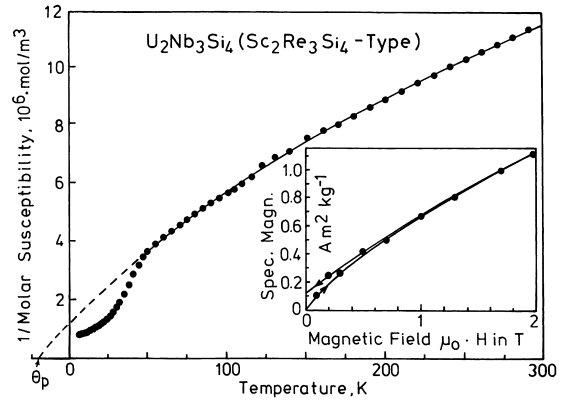

Fig. 7. Reciprocal susceptibility for $U_2Nb_3Si_4$ ($Sc_2Re_3Si_4$-type) and magnetisation versus magnetic fields up to 2 T (inset).

reflects the $Sc_2Re_3Si_4$-type. Occupancies have been refined for all atom sites revealing no deviation from the atom distribution given. Due to the usually strong correlation between occupational and thermal parameters, the isotropic temperature coefficients were individually analysed and kept constant throughout the refinement. The final structure and profile parameters and the reliability values obtained from the least squares refinements are presented in Table 4 including interatomic distances. Data in Table 4 were made consistent with a standardised setting of the atom positions employing the program *Structure Tidy* [17].

3.3.2. $U_{2-x}Nb_{3+x}Si_4$ with the ordered $Ce_2Sc_3Si_4$-type

The X-ray powder pattern of an alloy with the nominal composition $U_{20}Nb_{35}Si_{45}$ (in at.%), annealed and quenched from 1000°C, revealed a fairly homogeneous pattern but of a different structure type than the one observed at the composition $U_{22}Nb_{33}Si_{45}$ (in at.%) for stoichiometric $U_2Nb_3Si_4$. Retarded reaction kinetics prevented the formation of a single-phase product even after long term annealing treatments (up to 3000 h) still revealing significant amounts of $U_2Nb_3Si_4$ with the $Sc_2Re_3Si_4$-type and of α-Nb_5Si_3. Due to this fact and in view of the large quantity of overlapping reflections of the two structure modifications, we did not attempt to employ Rietveld refinement nor magnetic susceptibility measurements. Subtracting the secondary phases, the X-ray Guinier pattern, however, was completely indexed on the basis of a primitive orthorhombic unit cell. Extinctions observed for $(0\,k\,l)$, $k+l=2n+1$ and $(h\,0\,0)$, $h=2n+1$, respectively, are consistent with Pnma as the highest symmetric space group. The chemical formula, the unit cell dimensions, crystal symmetry and X-ray intensities are all compatible with the Sm_5Ge_4-type with only a small deviation ($U_{2-x}Nb_{3+x}Si_4$, $x \sim 0.25$) from a full atom order as for the $Ce_2Sc_3Si_4$-type, Ref. [16].

3.4. Magnetism

The magnetic properties of $U_2Nb_3Si_4$ ($Sc_2Re_3Si_4$-type) were investigated on a SQUID magnetometer in the temperature range 5–300 K and in fields up to 2 T. The inverse susceptibility could be fitted in the temperature interval 80–300 K using the modified Curie–Weiss law $\chi = (C/(T-\Theta_p)) + \chi_0$ with an effective paramagnetic moment $\mu_{eff} = 2.34\ \mu_B$/U atom, the paramagnetic Curie temperature $\Theta_p = -21$ K and a temperature independent term $\chi_0 = 33.9 \times 10^{-9}$ m^3/mol. Weak ferromagnetic interactions were observed below $\simeq$35 K; the magnetisation curve (see inset in Fig. 7) reveals a remanence of 0.0088 μ_B/U atom. None of the possible impurities from the binary boundary phases (see i.e., Ref. [3]) are magnetically ordered, therefore this behaviour is assumed to be intrinsic. Considering the negative paramagnetic Curie temperature the magnetic structure should essentially be antiferromagnetic, but a neutron powder diffraction experiment at 1.4 K failed to reveal any magnetic contribution (see inset in Fig. 6), which suggests that the magnetic moments are certainly smaller than $\approx 0.3\mu_B$.

4. Conclusion

Phase relations in the ternary system Nb–Si–U, established for the isothermal sections at 1000°C and 850°C, are characterised by the formation of two ternary compounds: stoichiometric $U_2Nb_3Si_4$ ($Sc_2Re_3Si_4$-type) and closely related $U_{2-x}Nb_{3+x}Si_4$, $x \simeq 0.25$ with the partially ordered Sm_5Ge_4-type ($Ce_2Sc_3Si_4$-type). The occurrence of these structure types is in line with the observations in the ternary uranium silicide systems with neighbouring T-elements [1], but is also consistent with

the formation of rare earth containing compounds $RE_2Nb_3Si(Ge)_4$ [2]. The observed two-phase equilibria: γ-(U,Nb) + $U_2Nb_3Si_4$ and Nb_5Si_3 + γ-(U,Nb) prove, that there is no compatibility between U_3Si_2 fuel and niobium metal at 1000°C and at 850°C, respectively. $U_2Nb_3Si_4$ is weakly ferromagnetic below $T_c \simeq 35$ K with a rather small remanence of only 0.0088 μ_B/U atom.

Acknowledgements

This research was in part sponsored by the European Union as a Human Capital and Mobility Network ERBCHRXCT930284. P.R. wishes to thank the Austrian National Science Foundation (Fonds zur Förderung der Wissenschaftlichen Forschung in Österreich) for support under grant P8218. The authors are thankful to M. Bohn from CNRS-URA 1278, IFREMER for the XMA measurements and to G. André, Saclay for the low temperature neutron diffraction experiment. T.L. is grateful to the French–Austrian Programme for Technical-Scientific Exchange for a research scholarship in Vienna (project A11).

References

[1] T. LeBihan, H. Noël, P. Rogl, J. Alloys Compounds 213/214 (1994) 540.
[2] T. LeBihan, K. Hiebl, P. Rogl, H. Noël, J. Alloys Compounds 235 (1996) 80.
[3] A. Zelinsky, Y.N. Grin, K. Hiebl, P. Rogl, H. Noël, G. Hilscher, G. Schaudy, J. Magn. Magn. Mater. 139 (1995) 23.
[4] J.A. Straatmann, N.F. Neumann, Equilibrium structures in the high uranium–silicon alloy system, USAEC Report MCW1486, Mallinckrodt Chemical Works, 23 October 1964, as cited in Reactor Materials, 8 (2) 1965 57.
[5] U.S. Nuclear Regulatory Commission Report, NUREG-1313, July 1988.
[6] K. Remschnig, T. LeBihan, H. Noël, P. Rogl, J. Solid State Chem. 97 (1992) 391.
[7] M.C. Bellisent-Funel, Neutron News 3 (1) (1992) 7.
[8] J. Rodriguez-Carvajal, Fullprof: a Program for Rietveld Refinement and Pattern Matching Analysis, Abstracts of the Satellite Meeting on Powder Diffraction of the XV Congress of the Int. Union of Crystallogr., Toulouse, France, 1990.
[9] V.F. Sears, In: R. Celotta, J. Levine, (Eds.), Methods of Experimental Physics, Neutron Scattering, 23, Part A, Academic Press, Orlando, FL, 1988, p. 521.
[10] L. Pouchou, F. Pichoir, J. Microsc. Spectrosc. Electron. 10 (1985) 279.
[11] B.T. Massalski, Binary Alloy Phase Diagrams, ASM, Materials Park, OH, 1990.
[12] M. Schlesinger, H. Okamoto, A.B. Gokhale, R. Abbaschian, J. Phase Equilibria 14 (1993) 502.
[13] S. Okada, K. Okita, K. Hamano, T. Lundström, High Temp. Mater. Proc. 13 (1994) 311.
[14] V. Sechovsky, L. Havela, in: E.P. Wohlfahrt, K.H.J. Buschow (Eds.), Ferromagnetic Materials, 4, Elsevier, Amsterdam, 1988, p. 309.
[15] V.K. Pecharskii, O.I. Bodak, E.I. Gladyshevskii, Dokl. Akad. Nauk Ukr. RSR A 40 (1978) 755.
[16] I.R. Mokraya, O.I. Bodak, E.I. Gladyshevskii, Sov. Phys. Crystallogr. 24 (1979) 729.
[17] E. Parthé, L. Gelato, B. Chabot, M. Penzo, K. Cenzual, R.Gladyshevskii, Typix-Standardized Data and Crystal Chemical Characterization of Inorganic Structure Types, Gmelin Handbook of Inorganic and Organometallic Chemistry, VIII ed., 1–4, Springer, Berlin, 1994.
[18] H. Holleck, H. Kleykamp, in: Gmelin-Handbook of Inorganic Chemistry, Uranium, Supplement, C12, Springer, New York, 1987 pp. 1–279.
[19] P. Villars, L.D. Calvert, Pearson's Handbook of Crystallographic Data for Intermetallic Phases, ASM, Materials Park, OH, 1991.
[20] I. Engström, B. Lönnberg, J. Appl. Phys. 63 (1988) 4476.
[21] T. LeBihan, thesis, Université de Rennes, France, 1993, pp. 1–194.
[22] P.L. Blum, G. Silvestre, H. Vaugoyeau, C. R. Acad. Sci. Paris 260 (1965) 5538.
[23] G. Kimmel, B. Sharon, M. Rosen, Acta Crystallogr. B 36 (1989) 2386.
[24] H. Noël, V. Queneau, J.P. Durand, P. Colomb, Abstract of a paper at Internl. Conf. on Strongly Correlated Electron Systems-SCES98, 15–18 July Paris, 1998, p. 92.